REPORT DOCUMENTATION PAGE

Form Approved
OMB NO. 0704-0188

1. AGENCY USE ONLY (Leave Blank)	2. REPORT DATE January 2004	3. REPORT TYPE AND DATES COVERED Peer Reviewed Reprint

4. TITLE AND SUBTITLE
Design and Characterization of MEMS Optical Microphone for Aeroacoustic Measurement

5. FUNDING NUMBERS
DAAD19-00-1-0002

6. AUTHOR(S)
K. Kadirvel, R. Taylor, S. Horowitz, L. Hunt, M. Sheplak, T. Nishida

7. PERFORMING ORGANIZATION NAME(S) AND ADDRESS(ES)
University of Florida, Gainesville, Florida 32611

8. PERFORMING ORGANIZATION REPORT NUMBER

9. SPONSORING / MONITORING AGENCY NAME(S) AND ADDRESS(ES)
U. S. Army Research Office
P.O. Box 12211
Research Triangle Park, NC 27709-2211

10. SPONSORING / MONITORING AGENCY REPORT NUMBER
40422, 3 - MS

11. SUPPLEMENTARY NOTES
The views, opinions and/or findings contained in this report are those of the author(s) and should not be construed as an official Department of the Army position, policy or decision, unless so designated by other documentation.

12 a. DISTRIBUTION / AVAILABILITY STATEMENT
Approved for public release; distribution unlimited.

12 b. DISTRIBUTION CODE

13. ABSTRACT (Maximum 200 words)

This paper presents the design and characterization of an intensity modulated optical lever microphone. Optical microphones (OM) have an inherent immunity to environments hostile to electronics due to the spatial separation of the electronics and the acoustic field under test. Theoretical equations for the sensitivity, minimum detectable signal, and frequency response are presented. Physical phenomena responsible for limiting the microphone minimum detectable signal (MDS) are identified, and a model is developed for use with a laser diode as the light source. The characterization of the microphone indicates an overall sensitivity of 0.5 mV/Pa, a linear response up to 132dB ref. 20 uPa, and an overall noise floor of 70dB measured at 1kHz over a 1Hz bin.

14. SUBJECT TERMS
MEMS
Optical microphone
Aeroacoustics

15. NUMBER OF PAGES
10

16. PRICE CODE

17. SECURITY CLASSIFICATION OR REPORT	18. SECURITY CLASSIFICATION ON THIS PAGE	19. SECURITY CLASSIFICATION OF ABSTRACT	20. LIMITATION OF ABSTRACT
UNCLASSIFIED	UNCLASSIFIED	UNCLASSIFIED	UL

NSN 7540-01-280-5500

Standard Form 298 (Rev.2-89)
Prescribed by ANSI Std. 239-18
298-102

AIAA 2004-1030

Design and Characterization of MEMS Optical Microphone for Aeroacoustic Measurement

Karthik Kadirvel, Robert Taylor, Steve Horowitz, Lee Hunt, Mark Sheplak, Toshikazu Nishida

University of Florida
Gainesville, FL

42nd Aerospace Sciences
Meeting & Exhibit
5-8 January 2004 / Reno, NV

Design and Characterization of MEMS Optical Microphone for Aeroacoustic Measurement

Karthik Kadirvel[1£], Robert Taylor[1£], Steve Horowitz[1£], Lee Hunt[2], Mark Sheplak[3§], Toshikazu Nishida[1&]

[1]Interdisciplinary Microsystems Group, Electrical & Computer Engineering, PO Box 116200, University of Florida, Gainesville, FL 32611 (352) 392-6774, (352) 392-0044 (FAX), nishida@ufl.edu
[2]Naval Surface Warfare Center, Panama City, FL 32407-7001
[3]Interdisciplinary Microsystems Group, Mechanical and Aerospace Engineering, University of Florida, Gainesville, FL

1. Abstract

This paper presents the design and characterization of an intensity modulated optical lever microphone. Optical microphones (OM) have an inherent immunity to environments hostile to electronics due to the spatial separation of the electronics and the acoustic field under test.

Theoretical equations for the sensitivity, minimum detectable signal, and frequency response are presented. Physical phenomena responsible for limiting the microphone minimum detectable signal (MDS) are identified, and a model is developed for use with a laser diode as the light source.

The characterization of the microphone indicates an overall sensitivity of *0.5 mV/Pa*, a linear response up to *132dB ref. 20 uPa*, and an overall noise floor of *70dB* measured at *1kHz* over a *1Hz* bin.

2. Introduction

A microphone is a transducer that converts acoustical energy into electrical energy. Microphones can be classified based on the transduction mechanism used to convert the signal from the acoustic domain to the electrical domain. In a traditional microphone, the transduction mechanism can be electrodynamic, piezoelectric, piezoresistive or capacitive. The electronics in a traditional microphone are co-located with respect to the acoustic field under test. In an OM, the acoustic signal is first converted to the optical domain before it is converted to the electrical domain. This allows the detection electronics to be remotely located with respect to the acoustic field, providing immunity of an optical microphone to environments harsh or damaging to electronics.

An optical microphone may use intensity modulation, phase modulation, or polarization modulation as the optical domain transduction mechanism [1]. Removing optical power from the optical path varies the light intensity in an intensity-modulated microphone. In a phase modulation OM, optical interference is used to modulate the optical intensity in the optical path. Polarization modulation microphones vary the polarization state of the light in the optical path and use polarization selective optics to vary the optical intensity incident on a photodiode. Since all photodiodes respond to optical intensity, any optical modulation strategy will require a variation in optical intensity received at a photo detector to properly convert the signal into the electrical domain.

Intensity modulated optical microphones are the simplest type of optical microphones. They can be fabricated using either microelectromechanical systems (MEMS) [2] or non-MEMS [3] technologies. In this paper, an intensity modulated, normal incidence lever MEMS OM, has been designed, fabricated, and characterized. The mechanical displacement of a MEMS diaphragm is used to modify the characteristics of the reflected light. The OM is theoretically analyzed and experimentally characterized.

A system overview will discuss the transduction stages as well as the microphone structure.

3. System Overview

3.1. Transduction Stages

An intensity-modulated lever microphone can be partitioned into three stages where transduction between energy domains occur [1]. They are the acousto-mechanical stage, the mechano-optical stage, and the opto-electrical stage.

£ Graduate Student
& Associate Professor
§ Associate Professor, Member AIAA

The acousto-mechanical transduction stage is where the energy in the acoustic signal is converted into the mechanical domain. This is accomplished when the pressure fluctuations of the acoustic signal induce a displacement in the membrane. The sensitivity (S_{am}) for this stage is displacement per unit pressure, given in μm/Pa.

In the mechano-optical stage, incident transmit (Tx) optical power reflected by the displacing membrane is coupled into the output receive (Rx) fibers. Transduction occurs when the mechanical displacement of the membrane varies the amount of input optical power that is coupled into the output fibers. The sensitivity (S_{mo}) of this stage is the input normalized output optical power per unit displacement, given in W/W/μm.

The final transduction stage in an intensity modulated OM is the opto-electrical stage. This stage uses one or more photodiodes to convert the coupled optical power into an electrical signal. Typically, a trans-impedance amplifier is included with the photodiode in the photo detector package. The sensitivity (S_{oe}) of this stage is the output voltage per normalized incident optical power, given in V/W/W.

3.2. Microphone Structure

The optical microphone structure consists of a MEMS diaphragm and an optical fiber bundle as shown in Figure 1.

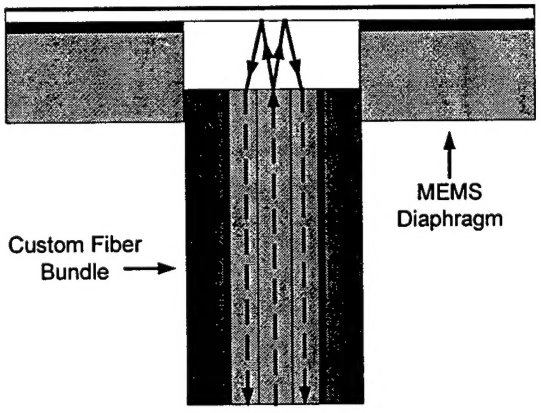

Figure 1. Optical microphone structure.

3.2.1. MEMS Diaphragm

The MEMS diaphragm consists of a *1mm* diameter, *1μm* thick silicon nitride membrane, coated with an *80nm* thick layer of aluminum to increase membrane reflectivity. Figure 2 shows a cross section of the MEMS diaphragm chip.

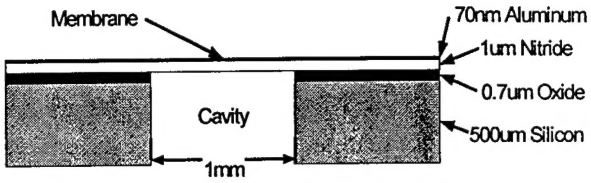

Figure 2. Cross section of MEMS diaphragm.

A fiber bundle is placed in the cavity at an optimal distance from the membrane where the slope of the optical coupling factor is maximum (section 4.1.2). An acoustic signal causes a displacement in the position of the membrane with respect to the end face of the fiber bundle, varying the amount of light collected by the receive fibers.

3.2.2. Fiber Bundle

The fiber bundle (Figure 3) consists of seven Thorlabs AFS105/125Y multimode fibers. These fibers have a core diameter of *105μm*, a cladding thickness of *10μm*, and a numerical aperture of *0.22*.

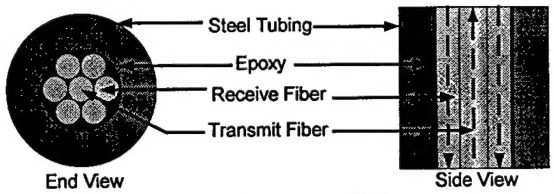

Figure 3. End face of the fiber bundle.

The seven fibers are inserted into an *825um* O.D., *400um* I.D. stainless steel hypodermic needle, cleaved and polished flush to the end. The center fiber is the transmit (Tx) fiber, which is connected to the light source. The six outer receive fibers (Rx) form a ring around the central transmit fiber.

3.3 Configurations

Two electronic configurations may be used to experimentally implement the OM, referenced and unreferenced (section 4.1.3). The unreferenced setup does not account for fluctuations in the laser optical power, but does provide a simpler implementation. The referenced setup uses an optical splitter and analog divide circuit to normalize the output with the input optical power. By minimizing any correlated optical power fluctuations, the minimum detectable acoustic signal (MDS) may be reduced.

4. Model of the Optical Microphone

A theoretical model to predict the sensitivity, frequency response, and minimum detectable signal has been developed for the OM.

4.1. Sensitivity

The overall system sensitivity of the OM is defined as the change in output voltage per change in input acoustic pressure. Each individual transduction stage has a sensitivity defined as the change in the stage output divided by the change in the stage input. The overall sensitivity of the OM is the product of the individual stage sensitivities.

4.1.1. Acousto-Mechanical Sensitivity

The acousto-mechanical stage converts input pressure fluctuations, p, into a displacement, w. The sensitivity of the stage is given by:

$$S_{am}(w) = \frac{\partial w}{\partial p}, \tag{1}$$

where w depends on the geometry and material properties of the circular plate.

In the case of a membrane, where k is the tension parameter, E the Young's modulus, h the membrane thickness, a the radius of the membrane, the transverse deflection w, as a function of radius r at an incident pressure p, is given by [4]

$$w(r) = \frac{2.78pa^4}{Eh^3k^2}\left[1 - \frac{r^2}{a^2}\right] \tag{2}$$

where k is given by

$$k = \frac{a}{h}\sqrt{\frac{12(1-\nu^2)\sigma_0}{E}}. \tag{3}.$$

If the light spot on the membrane is small (20% or less) with respect to the membrane diameter, then the sensitivity of the membrane can be lumped at the radial center. In this case, the acousto-mechanical sensitivity of the membrane, lumped at the radial center ($r=0$) is given by

$$S_{am} \equiv S_{am}(0) = \frac{2.78a^4}{Eh^3k^2}. \tag{4}$$

For the microphone designed, $a = 500um$, $h=1um$, Poisson's ratio $\nu=0.27$, in-plane stress $\sigma_0 \approx 65MPa$, and $E = 270GPa$. Using these dimensions and material properties, the acousto-mechanical sensitivity is approximately $1nm/Pa$.

4.1.2. Mechano-Optical Sensitivity

The pressure-induced displacement of the membrane modulates the reflected optical power, P_{mod}. The ratio of the modulated optical power to the input power, P_{in}, is defined as the optical power coupling factor, η. In the method of images (Figure 4), the reflecting surface is defined to be the reflecting plane, and the surface of the fiber bundle is defined to be the receiving plane.

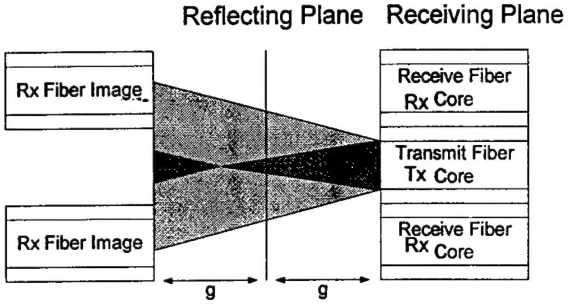

Figure 4. Method of images.

The planes are separated by a gap, g. The method of images states that the reflected optical power incident onto the Rx cores is the same as the optical power incident on the Rx core images, located at a distance of 2g from the receiving plane. The sensitivity of the mechano-optical stage is given by

$$S_{mo}(g) = \frac{d\eta}{dg}. \tag{5}$$

He and Cuomo [5] derived a formula for the optical power coupling factor by determining the light reflected from a deflected membrane in an optical lever microphone when multimode optical fibers are used to transmit and receive light. They determined the optical power coupled by using a ring approximation as shown in Figure 5.

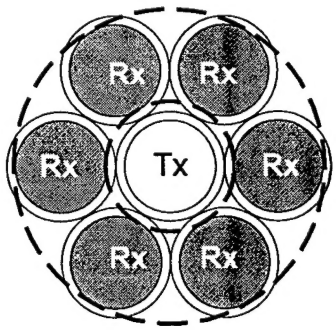

Figure 5. Ring Approximation used by He and Cuomo [5].

In [5], the receive fibers (core shaded grey) are assumed to form a perfect ring around the transmit fiber (core shaded white). Using this approximation, it is possible to relate the power coupled into the

receive fibers to the distance from the reflecting surface, 2g.

In their formulation, the irradiance is given by I_k, where k is the normalized radii, m is the relationship between the size of the core and the size of the cladding given by

$$m = 2 + \frac{R_{cladding} - R_{core}}{R_{core}}, \quad (6)$$

and σ is a normalization factor given by

$$\sigma = \cos^{-1}\left(\frac{k^2 + m^2 - 1}{2km}\right). \quad (7)$$

The optical power coupling factor is given by [5]

$$\eta(k) = \frac{P_{out}}{P_{in}} = \frac{2}{\pi}\int_{m-1}^{b} I_k \sigma k dk. \quad (8)$$

The optical power coupling factor versus gap distance is plotted and shown in Figure 6.

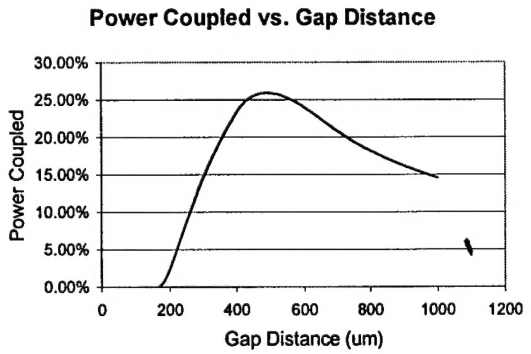

Figure 6. Power coupled vs. gap distance.

The slope of the optical power coupling factor curve gives the theoretical sensitivity of the mechano-optical stage. The optimum operating gap distance corresponds to the point of maximum slope. For the fiber bundle employed, the maximum slope occurs at a gap distance of 230 um:

$$S_{mo} = 1*10^{-3}\frac{W/W}{um}. \quad (9)$$

In the normal incidence configuration, the low mechano-optical sensitivity is due to the small divergence angle of the transmit fiber and large component of back-reflected light. A tradeoff exists between the microphone size determined by the fiber orientation (normal vs. oblique incidence) and the sensitivity. Normal incidence allows for a smaller sensor size.

4.1.3. Opto-Electrical Sensitivity

The opto-electrical transduction is accomplished with the use of a photo detector consisting of a photodiode and a trans-impedance amplifier. The sensitivity of the stage is given by the change is output voltage vs. the change in optical coupling factor

$$S_{oe} = \frac{dV}{d\eta}. \quad (10)$$

The output voltage of the opto-electrical stage is dependent on the detection electronics and the configuration used. The unreferenced opto-electrical configuration (Figure 7) uses one photo detector, and the referenced opto-electrical configuration (Figure 8) uses the ratio of two photo detector outputs.

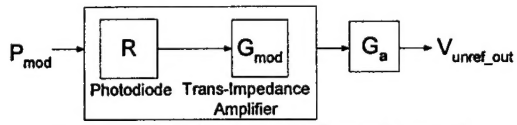

Figure 7. Block diagram of unreferenced configuration.

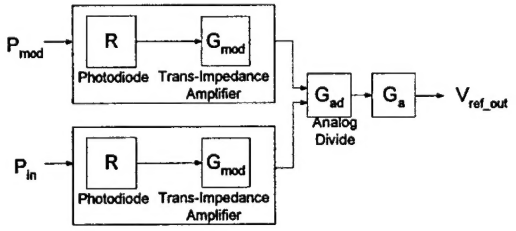

Figure 8. Block diagram of referenced configuration.

For the unreferenced detection configuration, the output voltage is a function of the photo detector responsivity (R), the trans-impedance gain (G_{mod}), pre-amp game (G_a), and the light source power (P_{in}) where P_{in} is assumed to be constant. The output voltage of the unreferenced opto-electrical configuration is given by

$$V_{unref\_out} = RG_{mod}G_aP_{mod} = RG_{mod}G_aP_{in}\eta. \quad (11)$$

The sensitivity of the unreferenced opto-electrical stage is described by

$$S_{oe\_unref} = RG_{mod}G_aP_{in}. \quad (12)$$

In the referenced configuration, an analog divide circuit is used to compare the modulated optical output power (P_{mod}) to the reference input optical

power (P_{in}). The referenced output voltage can be shown to be the following

$$V_{ref\_out} = G_{ad} G_a \left(\frac{R G_{\mathrm{mod}} P_{\mathrm{mod}}}{R G_{in} P_{in}} \right) \qquad (13)$$

where the gain of the analog divide block is G_{ad}. Since P_{in} is measured, the referenced configuration can minimize the effect of input power fluctuations on the modulated output power. The referenced output voltage can be simplified to the following assuming identical responsitivity for the two photo-detectors

$$V_{out} = G_{ad} G_a \left(\frac{G_{\mathrm{mod}}}{G_{ref}} \right) \eta . \qquad (14)$$

The opto electrical sensitivity of the referenced optical microphone is then given by

$$S_{oe\_ref} = G_{ad} G_a \left(\frac{G_{\mathrm{mod}}}{G_{ref}} \right). \qquad (15)$$

4.2. Minimum Detectable Signal

The minimum detectable signal (MDS) is the smallest acoustic signal that can be resolved by the optical microphone within a given bandwidth at a specific frequency. It is a function of the noise sources in the three stages and the stage sensitivities.

The dominant noise source in the acousto-mechanical stage is due to dissipative mechanisms through the fluctuation-dissipation theorem [6]. The operative dissipation mechanisms involve energy transfer through intrinsic and extrinsic molecular agitations. External molecular interactions include Brownian motion, viscous damping, and acoustic radiation while internal interactions include thermoelastic damping in the membrane or supports. In analogy with lumped electrical systems, a dissipater in the acoustic domain may be modeled as an acoustic resistance, R_a. The corresponding average spectral density of pressure fluctuations, $<p_{AM}>$, is given by the Nyquist relation

$$< p_{AM} >= \sqrt{4 k_B T R_a} . \qquad (16)$$

in units of [Pa/√Hz] where k_B is the Boltzmann constant and T is the temperature in degrees Kelvin.

Not all of the mechanical dissipation mechanisms are well characterized. However, consider the mechanical radiation resistance for a circular piston in a semi-infinite baffle. The mechanical radiation resistance is given by [7]

$$R_{rm} \cong \frac{1}{2} \pi a^2 \rho_0 c (ka)^2 \ for\ ka << 1 \qquad (17)$$

where k is the acoustic wave number, ρ_0 is the density of air, and c is the speed of sound. The radiation resistance in the acoustic domain is given by

$$R_{ra} = \frac{R_{rm}}{A^2}, \qquad (18)$$

where A is the effective diaphragm area to maintain the continuity of the volume velocity [8]. For this example, the resulting pressure fluctuation is negligible compared to the optical and electrical noise sources.

The dominant noise source in the mechano-optical stage is the intensity noise of the light source. The optical power coupled into the receive fibers can be written as the sum of the d.c. component of the light source intensity, I_{light}, the time-varying optical intensity fluctuations, $I_{light\_noise}(t)$, and the time-varying optical intensity modulation, $I_{mod}(t)$, resulting from the desired acoustic signal. The intensity terms are converted to an optical power by integration over a surface area. Optical intensity fluctuations may be significant for a laser diode source, particularly in the presence of back-scattered light.

Both light source intensity noise and the inherent noise of electrical components are present in the OE stage and can affect the OE MDS. Previous optical microphone noise studies (He and Cuomo 1991 [5], 1992 [9]) acknowledge the presence of light source intensity noise, but only consider the photodiode shot noise in theoretical models. While photodiode shot noise is the dominant noise source generated in the electrical domain, the optical noise power incident on the active area of the photodiode can also be significant, and should be included in an overall model for the optical microphone MDS. The equation for the optical microphone MDS, in terms of the individual stage MDS, is given by

$$MDS = \sqrt{MDS_{AM}{}^2 + MDS_{MO}{}^2 + MDS_{OE}{}^2} \qquad (19)$$

in units of [Pa/√Hz] where the acousto-mechanical stage MDS is modeled by (16), and the mechano-optical and opto-electrical MDS are given by

$$MDS_{MO} = \frac{\left\langle \frac{P_{light\_noise}}{P_{light}} \right\rangle}{S_{am} S_{mo}} \qquad (20)$$

and

$$MDS_{OE} = \frac{\langle V_{oe} \rangle}{S_{am} S_{mo} S_{oe}}, \qquad (21)$$

respectively. V_{oe} represents either the unreferenced output voltage fluctuations, V_{oe_unref}, or the referenced output voltage fluctuations, V_{oe_ref}, whichever is applicable. The average spectral density of shot noise-induced voltage fluctuations is given by

$$<V_{oe\_detector}> = G\sqrt{2eRP_{light}} \qquad (22)$$

where G is the detector trans-impedance gain.

4.3. Frequency Response

The overall MEMS OM frequency response is modeled using a lumped equivalent model (LEM) shown in Figure 9.

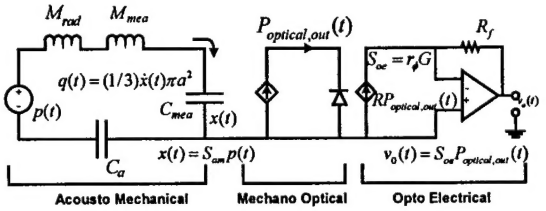

Figure 9. Lumped element model/equivalent electrical circuit.

As discussed previously, the MEMS OM may be partitioned into three stages: AM, MO, and OE. Using a LEM for each of the stages, H_{am}, H_{mo}, and H_{oe}, the overall frequency response is given by:

$$H(s) = \left\{\frac{1}{1+s^2 C_{eff} M_{eff}}\right\}\{1\}\left\{\frac{1}{\frac{s}{2\pi f_{cut\,off}}+1}\right\} \quad .(23)$$

The general mechanical deflection of the diaphragm for an incident pressure is governed by plate theory. The behavior of the diaphragm may be approximated, i.e. lumped as an effective mass and effective compliance, when the device scale of interest, *D*, is much smaller than the characteristic length of the physical phenomenon, in this case the acoustic wavelength, λ (1.7 cm at 20 *kHz* and 33 cm at 1 *kHz*). This criterion is met for the frequencies of interest, $D << \lambda$. In the acoustic domain, the distributed kinetic energy of the membrane is modeled as a lumped kinetic energy corresponding to an effective mass M_{mea} at $r = 0$. Similarly, the distributed potential energy is approximated as a lumped potential energy corresponding to an effective compliance C_{mea} . The effective mass of the air particles moving with the membrane is modeled by a radiation mass, M_{rad} . The cavity impedes the motion of the diaphragm by storing potential energy and is modeled as an effective acoustic cavity compliance, C_a .

The model parameters developed in terms of the structural parameters are evaluated and listed in Table 1.

Table 1. Lumped element model parameters.

Parameter	Formula	Value
M_{mea}	$\frac{\rho_n h}{3\pi a^2}$	$1.188\cdot10^3 \frac{kg}{m^4}$
C_{mea}	$\frac{\pi a^4}{2\sigma_o h}$	$1.15\cdot10^{-15} \frac{m^3}{Pa}$
M_{rad}	$\frac{\rho_a}{3\pi a^2}$	$661.965 \frac{kg}{m^4}$
C_a	$\frac{\pi a^2 h_{cav}}{\rho_a c}$	$1.764\cdot10^{-15} \frac{m^3}{Pa}$

The theoretical frequency response plot for the OM is shown in Figure 10, normalized to the static sensitivity.

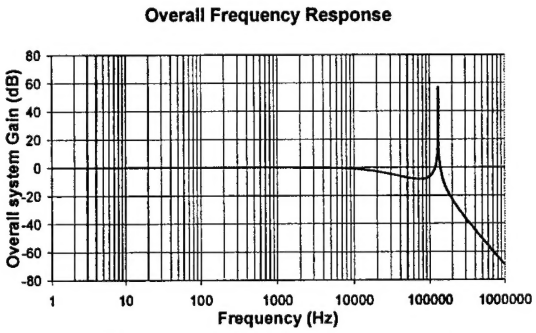

Figure 10. Frequency response of optical microphone system normalized to the static sensitivity.

5. MEMS Diaphragm Fabrication

The MEMS diaphragm was fabricated using the MEMS Exchange foundry. The key steps of the process flow are shown in Figure 11.

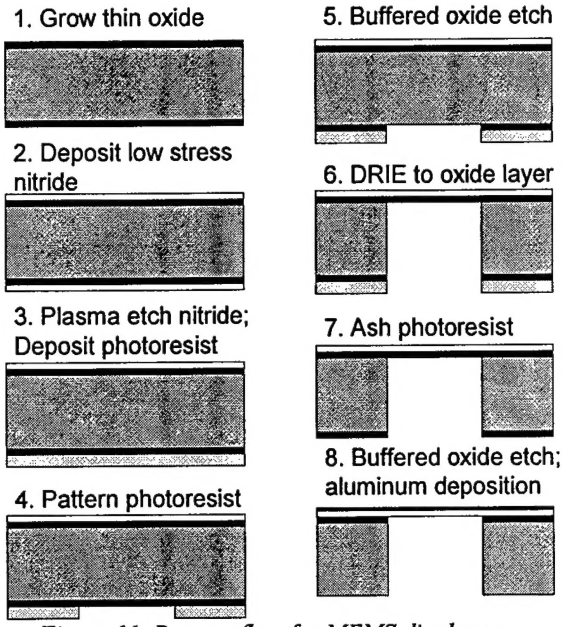

Figure 11. Process flow for MEMS diaphragm.

6. Experimental Characterization of the Optical Microphone System

6.1. Experimental Setup

In the setup, a Hewlett Packard tunable laser source at *1550nm* and Thorlabs PDA-400 photo detectors with trans-impedance gain, $G = 1.5x10^5$ *V/A* and responsitivity, $R = 0.95$ *A/W* were used. In addition a low noise SR560 pre-amp was used at the output. The pre-amp was configured as a highpass filter with a cut-on frequency, f_o, of *30 Hz* and a voltage gain, $G_a = 10$ *V / V*.

6.2. Experimental Results

Preliminary data are presented for the unreferenced configuration using an input optical power of 250 μW at 1550 nm, R = 0.95 *A/W*, $G_{mod} = 1.5x10^5$ *A/V*, and $G_a = 10$ *V/V*.

6.2.1. Static Calibration

In the static calibration, a micropositioner was used to step the fiber bundle away from a mirror that is aligned normal to the bundle. The input power into the transmit fiber and the output power collected by the receive fiber bundle was measured, and the experimental optical power coupling factor curve was obtained.

Figure 12 plots the measured and theoretical output power coupling factor as a function of gap distance.

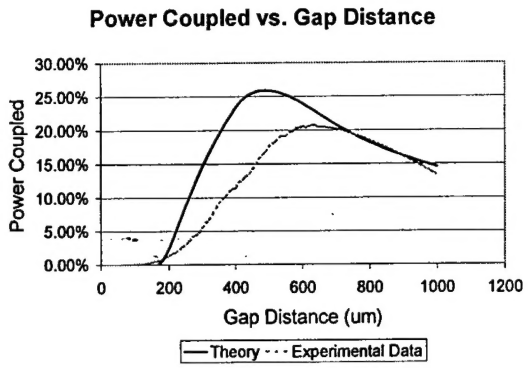

Figure 12. Static calibration curve.

The theoretical optical power coupling curve has a maximum slope of $1\times10^{-3} W/W/\mu m$ at $g = 230\mu m$ while the measured optical power coupling curve has a maximum slope of $8\times10^{-4} W/W/\mu m$ at $g = 360\mu m$. The mechano-optical sensitivity (slope of power coupling curve) is linear within 3% over the range *340um to 380um.*

The discrepancy between the two power coupling curves is attributed to fiber misalignment and positioning errors. Misalignment includes angular alignment errors where the fiber bundle is not perpendicular to the membrane. It also includes positional alignment errors between the transmit fiber and the center of the membrane. Based on the O.D. of the hypodermic tube (*825um*), membrane diameter (*1mm*), and the support plug length (*20mm*) an angular misalignment of *0.5* degrees is possible. The lateral misalignment could be as high as *88um* from the center transmit fiber to the center of the diaphragm. Position error is caused by the receive fibers not forming a tight ring around the transmit fiber. Clearly, these issues may be improved with MEMS fiber packaging techniques.

6.2.2. Dynamic Calibration

The dynamic calibration is conducted after the static calibration to ensure that the fiber bundle is at the optimal gap distance from the diaphragm. One method for calibrating microphones in a known acoustic field is the use of a plane wave tube (PWT). A PWT is a rigid-walled duct that supports planar acoustic waves propagating along the length of the duct. For linear lossless acoustic motion in a rigid-walled, square duct, the fundamental mode *(0,0)* plane wave propagates at all frequencies. The higher order modes are evanescent when the acoustic wavelength is greater than twice the width of the duct ($\lambda > 2D$). A 1" square duct PWT was used. Therefore, below the first cutoff frequency, $f < c_0 / 2D = 6.5$ *kHz*, the duct will propagate only plane

waves. Sensors installed at the same axial distance from the driver are assumed to sense the same field. This permits the calibration of a microphone when referenced to another microphone with a known response. A B&K 4138 reference microphone was mounted next to the optical microphone in the PWT. The frequency response was measured using a band limited periodic random noise signal up to 6.5 *kHz*.

The sensitivity of the microphone was measured using a single tone *1kHz* sine wave as the input. The sensitivity was measured to be *0.5 mV/Pa*, with a linear response to *132dB*. The theoretical sensitivity is approximately 0.3 mV/Pa. The under estimation of the sensitivity may be due to inaccuracies in the determination of the power coupling factor. The linearity of the optical microphone is shown in Figure 13.

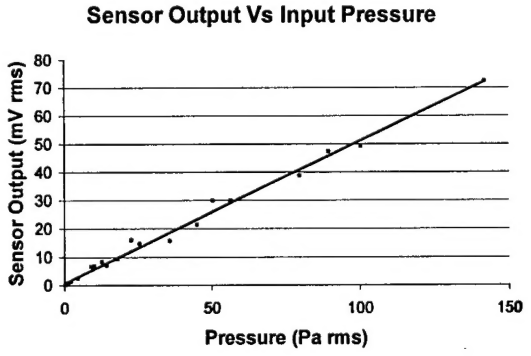

Figure 13. Linearity plot of optical microphone at 1kHz.

The magnitude frequency response of the optical microphone in the unreferenced configuration is shown in Figure 14.

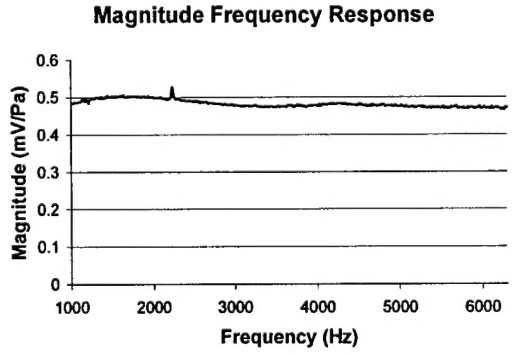

Figure 14. Magnitude frequency response of optical microphone.

The phase response of the unreferenced configuration is shown in Figure 15.

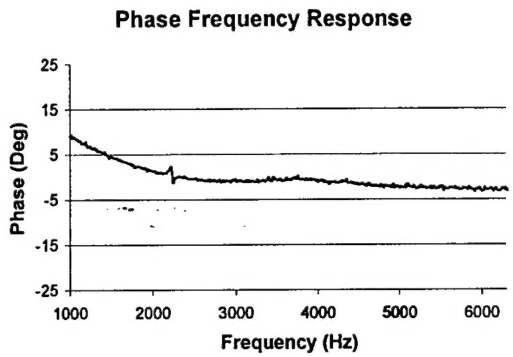

Figure 15. Phase response of optical microphone.

The preliminary noise floor of the optical microphone (Figure 16) is determined by measuring the output of the photo detector with no input acoustic signal at 1 *kHz* and 1 *Hz* frequency bin.

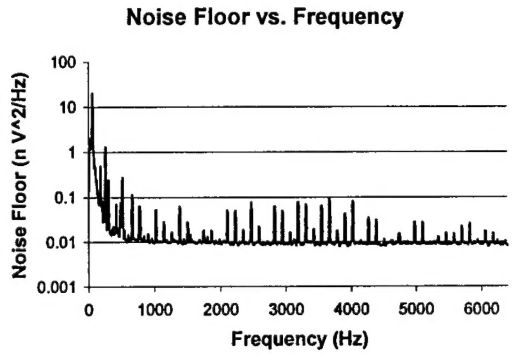

Figure 16. Noise floor of optical microphone.

The minimum detectable input signal is then found by dividing by the overall sensitivity. The preliminary minimum detectable signal for a *1Hz* frequency bin centered at *1kHz* is estimated to be *70 dB* referenced to $20\ \mu Pa$.

7. Conclusions

An optical microphone for aeroacoustic measurement immune to EMI has been designed, fabricated and characterized. Preliminary characterization indicates an overall sensitivity of *0.5 mV/Pa*, a linear response up to *132dB ref. 20* μPa, measured flat frequency response from *1kHz* to *6.4kHz*, and an overall noise floor of *70dB* measured at *1kHz* over a *1Hz* bin width.

Alignment and position issues indicate a need for improved packaging of the fiber bundle with the MEMS diaphragm. Improving the alignment and positioning will improve the performance of the

microphone. Another improvement can be made to the microphone by using a referenced electronic configuration to reduce optical source fluctuations.

Constraints and the theoretical equations presented here could be used to determine the optimal configuration and performance of the optical microphone when designed for specific end applications.

8. Acknowledgements

Financial support for this project was provided by DARPA (Grant #DAAD19-00-1-0002) through the Center for Materials in Sensors and Actuators (MINSA) and is monitored by Dr. Paul Holloway.

9. References

[1] N. Bilaniuk, "Optical Microphone Transduction Techniques," *Applied Acoustics*, vol. 50, pp. 35-63, 1997.

[2] "Surveillance Optical Microphone (SOM) Product Data Sheet," Phone-Or.

[3] G. He and F. W. Cuomo, "Displacement Response, Detection Limit, and Dynamic Range of Fiber-Optic Lever Sensors," *Journal of Lightwave Technology*, vol. 9, pp. 1618-1625, 1991.

[4] M. Sheplak and J. Dugundji, "Large Deflections of Clamped Circular Plates Under Initial Tension and Transistions to Membrane Behavior," *Journal Applied Mechanics*, vol. 65, pp. 107-115, 1998.

[5] G. He and F. W. Cuomo, "A Light Intensity Function Suitable for Multimode Fiber-Optic Sensors," *Journal of Lightwave Technology*, vol. 9, pp. 545-551, 1991.

[6] T. B. Gabrielson, "Mechanical-Thermal Noise in Micromechanical Acoustic and Vibration Sensors," *IEEE Transactions Electronic Devices*, vol. 10, pp. 903-909, 1993.

[7] L. E. Kinsler, A. R. Frey, A. B. Coppens, and J. V. Sanders, *Fundamentals of Acoustics*, 3 ed: John Wiley & Sons, 1982.

[8] M. Rossi, *Acoustics and Electroacoustics*: Artech House, 1988.

[9] G. He and F. W. Cuomo, "The Analysis of Noise in a Fiber Optic Microphone," *Journal of Acoustical Society of America*, vol. 92, pp. 2521-2526, 1992.